ELSEVIER

Journal of Nuclear Materials 241–243 (1997) 105–117

journal of nuclear materials

Impurity release and deposition processes close to limiter surfaces in TEXTOR-94

V. Philipps *, A. Pospieszczyk, H.G. Esser, U. Kögler, G. Mank, U. Samm, B. Schweer, J. von Seggern, B. Unterberg, E. Vietzke, F. Weschenfelder, P. Wienhold, J. Winter, the TEXTOR team

Institut für Plasmaphysik, Forschungszentrum Jülich, Ass. Euratom-KFA, 52428 Jülich, Germany

Abstract

Measurements on the formation of hydrocarbons on plasma exposed surfaces performed by mass- and optical emission spectroscopy in TEXTOR is reported. The temperature dependence of hydrocarbon formation and the contribution of the hydrocarbon source to the CII ion densities near the limiter has been observed using a graphite limiter which is externally heatable up to 1400 K. It has been found that hydrocarbon formation occurs in a broad temperature region decreasing only for target temperatures above 1300 K and that hydrocarbons contribute to about 40% to the CII light. Strong methane release has been observed on copper and stainless steel limiters positioned at the LCFS while it is negligible on molybdenum and tungsten limiters under similar plasma edge conditions. Local transport and redeposition of molecules have been studied by gas injection of methane and silane through holes in the limiter surfaces and by local Monte Carlo calculations. Local deposition efficiencies between 4 and 7% have been measured for injected methane and silane. Monte Carlo calculations show, in general, a larger redeposition probability depending only little on local plasma parameters but significantly on the assumptions of the sticking and release properties of redeposited ions and radicals on the surface. For higher surface temperatures possible carbon release by radiation enhanced sublimation (RES) has been investigated. No increase of carbon release could be observed demonstrating that carbon release from RES is negligible under these conditions. Possible reasons for this behavior are discussed.

Keywords: TEXTOR; Chemical erosion; Physical erosion; Erosion and particle deposition

1. Introduction

Reduction and control of the impurity influx to the core plasma and control of wall erosion are main issues for long pulse thermonuclear plasma devices. These issues require the knowledge of the different mechanism of impurity production under relevant particle impact conditions and a thorough understanding of the impurity transport in the vicinity of the target surfaces and in the main plasma. It is essential that the concepts to achieve these aims must be compatible with the requirements for helium ash and energy exhaust during extended burn times. As in the case of a radiative boundary, for example, they largely change the plasma edge conditions and thus influence the impurity production and wall erosion. They also will constrain the amount of intrinsic impurities in the plasma core.

To study the production of impurities and their local transport, a system of limiter locks has been developed in TEXTOR by which different limiters can be inserted into the plasma edge. A set of optical diagnostics observes these limiters both from the top and side. Graphite limiters have been developed which can be externally heated up to about 1300 K. Gas puffing through holes at different locations on the limiter surface is used to study local transport and redeposition under well defined particle source conditions.

* Corresponding author. Tel.: +49-2461 616 331; fax: +49-2461 612 660.

PII S0022-3115(96)00499-0

Physical sputtering is a universal mechanism of impurity production since it occurs for all wall materials independent of their chemical nature. Reduction of this impurity release channel requires low ion impact energies and large masses of the target material. In fact, in the concept of the high density divertor with low divertor plasma temperatures near 10 eV, or even below, physical sputtering is reduced significantly. The effect is most pronounced for heavy metals like molybdenum or tungsten and high-Z metals might be used under such conditions. Critical questions for their applicability are the efficiency of local screening of sputtered high-Z impurities, divertor retention and possible accumulation of high-Z in the plasma core [1].

The present experiences and database of tokamaks suggests that low-Z carbon materials offer a solution as a target material in the next step of fusion devices. Higher impurity concentration can be tolerated in the main plasma due to low radiation losses and radiation is emitted mostly from the outer plasma regions. These materials have good thermomechanical properties and they do not melt when exposed to off-normal heat loads.

The main concern with carbon materials are their large erosion rates. Physical sputtering reaches rather large values even at low impact energies. In addition they are eroded chemically by forming volatile hydrocarbons with the plasma fuel and oxides with residual oxygen plasma impurities. It has been shown that control of the residual oxygen concentration is essential to achieve fusion plasmas with high performance [2]. This is related to the fact that oxygen impurities react with carbon to form CO with a yield near unity [3]. Efficient ways to control were developed at TEXTOR by plasma assisted coating of the wall with oxygen getters like boron [4] or silicon [5]. Possibilities of oxygen gettering should also be foreseen in the next step fusion device. Chemical erosion by oxygen impact will not be discussed in this paper.

The importance of hydrocarbon formation for wall erosion and carbon contamination of the main plasma is not fully clear yet. The low energy and high flux conditions in front of the targets in fusion experiments can not be reproduced in beam experiments and absolute measurement of molecule formation in fusion experiments are needed. In particular in case of the high density, low energy divertor scenario hydrocarbon formation may dominate wall erosion and carbon impurity production. Of similar importance is analysis of the local transport and screening of the molecules. These processes have been studied by puffing methane and silane gas through holes in testlimiters and the ALT-II pumplimiter. A Monte Carlo code has been developed to study the transport of the molecules in the vicinity of the testlimiters. Some results will be shown in Section 4.

Ion beam experiments have shown that graphite shows an additional carbon release mechanism above about 1200 K, called radiation enhanced sublimation (RES) [6,7]. According to the beam data this mechanism should dominate carbon release in the temperature range from 1200 to 2000 K and is expected to limit the working temperatures of carbon based materials significantly. This would partly reduce the advantages of carbon as a high temperature material. Most of the observations on carbon release from targets in fusion devices have shown that this erosion is less dominant than predicted from beam experiments. However contradictory observations have been published [50] and further clarification is necessary. This erosion process will be discussed in Section 5.

Wall erosion and lifetime of wall components are a further concern with low-Z carbon materials. Estimates show that the primary erosion of carbon targets at the location of peak particle fluxes lead to unacceptably high material loss. Any target concept based on carbon therefore relies on the assumption that a large fraction of eroded material is redeposited close to its origin. Modeling of redeposition has been done for certain plasma and geometrical conditions but the predictions contain large uncertainties and more experimental work and deeper knowledge of the processes is necessary. Experimental investigations on redeposition properties are scarce but needed. In TEXTOR gas puffing has been used to measure in situ [8], and postmortem, the deposition efficiency of carbon and silicon injected via CH_4 and SiH_4, and the results have been compared with Monte Carlo calculations. Even more important is to develop methods to actively influence and control the processes of local erosion and redeposition. It has been demonstrated that gas puffing changes erosion dominated zones on the limiter to redeposition areas. This opens in principle the possibility to replace eroded material and to repair limiter surfaces. It has been found that deposition patterns of injected gases on the limiter surfaces are influenced by local electrical fields [40]. These effects must be included when the local redeposition behavior in fusion experiments is considered.

2. The limiter lock system

In TEXTOR-94, limiters up to a diameter of 14 cm can be introduced from the bottom and from the top of the machine using vacuum lock systems. Graphite limiters have been equipped with a resistively heated film from the backside. They reach surface temperatures of about 1400 K so far. Power loads have been determined by thermography performed by CCD cameras from the top. Thermocouples positioned 7 mm behind the surface near the location of maximum heat load allow reconstruction of the surface temperature and also determination of the overall deposited energy by using the limiter as a calorimeter. Impurity release or injection is studied from a side view using a spectrometer equipped as detector with a CCD camera and an image intensifier. The spectrometer provides radially resolved intensities at a fixed toroidal position and inte-

grates intensities in poloidal direction. Additionally a CCD camera equipped with interference filters views the total emission light from the side view and optionally from the top. From these data the toroidal distribution pattern of different ionization states in the vicinity of the limiter surfaces has been observed. High resolution spectroscopy is used to determine the velocity distributions of emitted species [9]. Gas puffing of methane, higher hydrocarbons, silane and hydrogen has been performed by calibrated gas inlets through holes drilled at different locations at the limiter surface to simulate particle sources of known intensity and to observe their radial and toroidal transport in the vicinity of the limiters. Different limiter materials have been investigated (C, B_4C, Cu, SS, Mo, W, Si–C etc) and initial results have been reported [10,11].

3. Hydrocarbon formation

Years of plasma wall interaction research in fusion devices have not determined clearly the importance of hydrocarbon formation for wall erosion and carbon contamination of the main plasma. In laboratory experiments hydrocarbon formation from carbon materials has been investigated intensively with thermal and energetic hydrogen beams and the main trends are, in general, consistent [12,13]. The chemical erosion of carbon by hydrogen impact is a rather complex process depending on surface temperature, ion flux density and energy and carbon material. For exposure of carbon to hydrogen atoms with thermal energies, a model of hydrocarbon formation has been developed which is based on the hydrogenation of unsaturated carbon bonds leading to the release of CH_3 radicals [14,15]. Similar processes are assumed for the interaction of energetic hydrogen, but additional collisional processes have to be taken into account. They can lead to bond-breaking, creating or destroying carbon bonds on which hydrogenation can appear. At temperatures lower than about 600 K and low impact energies, surface hydrocarbon complexes can also be ejected by collisional energy transfer. In fusion experiments hydrocarbon formation occurs under the impact of hydrogen ions at high fluxes and low energies with the simultaneous impact of low energy neutrals from charge-exchange and Franck–Condon processes. Monte Carlo calculations show that the neutral flux is about 15–30% of the impinging hydrogen ion flux for the conditions at the TEXTOR limiters. According to the present understanding [16] the importance of the collisional processes for hydrocarbon formation increase under these conditions compared with the thermally activated processes. This results in rather large hydrocarbon formation also at temperatures below 600 K, flattening thus the temperature peak of the chemical erosion. Laboratory experiments show [17,18] that low energy hydrogen neutrals lead to the emission of CH_3 radicals instead of saturated CH_4 and to preferential formation of higher C_2H_x hydrocarbons with a yield roughly twice that for methane. In addition, carbon impurities from the background plasma impinge on the surfaces, which will, depending on carbon impact energy and mass of the target, be directly reflected or stick on the surface. The sticked carbon atoms modify the surface composition and structure but may again be eroded by the plasma particles. They can, depending on the material, even lead to the formation of hydrocarbons on metallic limiters (see Section 3.4) underlining their possible importance for hydrocarbon formation. It is presently assumed that they will not influence the hydrocarbon formation on carbon materials, but this has not yet been determined.

3.1. Mass spectroscopy in TEXTOR

3.1.1. Methane

Hydrocarbon formation is measured in TEXTOR by mass spectroscopy of either the neutral gas pressure near the wall using conventional mass spectrometers, or with the Sniffer probe where higher fluxes and geometrically defined conditions are achieved [19]. This system acts as a small pump limiter unit positioned into the SOL typically > 1 cm behind the LCFS, in order to avoid excess heat flux. A plasma column of 4×7 mm impinges through an aperture in front of a tube onto a graphite strip, which can be heated by direct current. Hydrocarbons and recycled hydrogen built up a neutral gas pressure at the end of the tube that is sampled by a quadruple mass spectrometer. The schematic of the set-up and typical results are shown in Fig. 1. Hydrocarbon formation is deduced from the pressure rise which can be determined with good accuracy. The hydrocarbon molecules which are formed as well as recycled hydrogen at the target have to travel long distances before they are detected. They can thus interact with the plasma column in the tube as well as with the tube walls. We assume that formed radicals recombine at the chamber walls into saturated molecules and that their sticking to the walls is negligible. For the hydrogen atoms reflected from the target we assume recombination at the walls where they can also form hydrocarbons. Under standard TEXTOR conditions hydrogen ion flow in the SOL consists of a mixture of deuterium and hydrogen, depending on wall conditioning and fueling of the discharge. This leads methane formation containing mixed hydrogen isotopes (CH_4, CH_3D, CH_2D_2, CHD_3, CD_4). Interestingly the methane isotope fractions are determined by the relative fractions of H and D fluxes in the SOL assuming a reaction of 4th order. Ion fluxes on the target have been measured via the ion saturating current(-200 V biasing) and have been found to be typically 20–50% larger than the hydrogen fluxes evaluated from the hydrogenic pressure rise at the end of the tube. The data are in reasonable agreement and the differences can be understood by taking into account the charge contribution of impurity ions im-

pinging on the probe, leakage out of the aperture and experimental uncertainties.

Fig. 2 shows typical results for the methane formation. It shows the methane yield evaluated from the pressure ratios of methane to hydrogen during the flat top phase of ohmic and NBI heated discharges at different line averaged densities. The aperture of the probe is at $r = 48.7$ cm, 2.7 cm into the SOL (width of 0.4 cm). We know from several other observations in TEXTOR that under these conditions carbon and other impurities (boron/silicon) impinging on the target will build up a layer on the target thus that hydrocarbon formation occur on a kind of a mixture material. The left side shows the evaluated impinging hydrogen flux densities which range between 5×10^{17} and 5×10^{18} H,D/cm^2 s. Plasma temperatures at this radius are very low ($\approx$ 5–10 eV) at high plasma densities and near 20 eV at low densities. The figure demonstrates some typical findings: The methane yields evaluated from the pressures are between about 0.7 and 1.2% at target

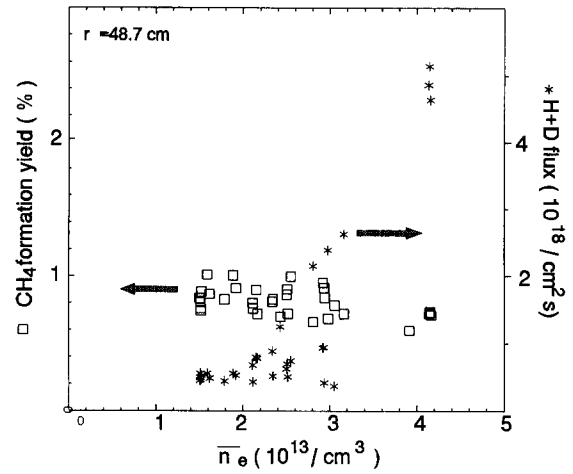

Fig. 2. Methane yields and hydrogen fluxes evaluated from the hydrogenic and methane pressure ratios with non heated graphite target ($T < 150$°C) versus line averaged density for ohmic and NBI heated discharges. The aperture of the tube is 2.7 cm inside the SOL.

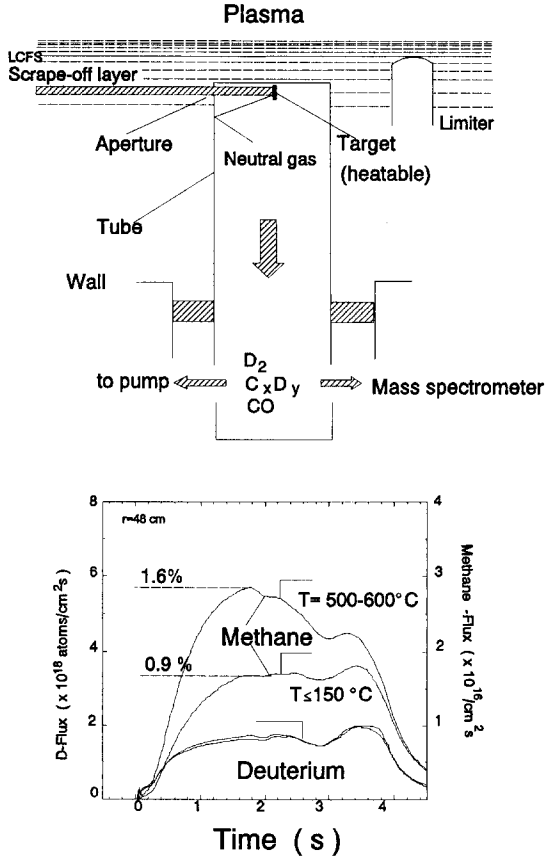

Fig. 1. Upper: Schematic of the Sniffer probe. Lower: Temporal evolution of the hydrogenic ($H_2 + HD + D_2$) and methane pressure (sum of $C_1H_xD_y$) measured in the Sniffer probe for two identical subsequent discharges, but with different target temperature. Hydrogen and methane fluxes are directly converted from the pressures using mass spectroscopic calibration factors.

temperatures below $\approx$ 500 K and do not depend much on plasma parameters and hydrogen flux densities. There is a only a weak tendency of decreasing yields with increasing flux density within this flux range. Similar yields have been obtained under many other conditions. Upon increasing the target temperature the yields increase by a factor between 1.5 and 2, as shown, for example, in the lower part of Fig. 1. However, the temperature of the target is not measured directly and target temperatures can only be given with some uncertainty.

An important question is whether wall conditioning, e.g., siliconization can reduce methane formation as it is observed in beam experiments [20]. The methane yields in TEXTOR have been observed to decrease only slightly and recover quickly to values measured before wall conditioning. Similar results are obtained by optical spectroscopy (Section 3.3). Deposition probe measurements performed after boronization/siliconization show typically a ratio of B,Si/C of about 1/1 (first day) in the deposited layers and the methane formation at the target is assumed to occur under similar material composition conditions. Thus significant amounts of boron and silicon in the deposited layers do not decrease the methane yields significantly. Any observed reduction is certainly much less compared with high energy hydrogen beam experiments on boron doped carbon materials. This behavior is also observed in PISCES [21] and during beam irradiation at low impact energy [22]. The measurements show that the beneficial effect of a reduced methane formation from doped carbon materials are reduced for low energy hydrogen impact. This shall be kept in mind when thinking about techniques to reduce carbon erosion in future devices.

3.1.2. Higher hydrocarbons

Beam experiments show that higher hydrocarbon formation is negligible for high hydrogen impact energies but their importance increases with decreasing impact energy [23]. Thermal hydrogen atoms impinging on amorphous a-C:H films show C_2H_x formation about twice that of methane [24].

Mass spectroscopy on C_2-hydrocarbon formation in TEXTOR is not as consistent as for methane, showing a much larger scatter under similar plasma conditions. Some of the scatter result from the complexity of the C_2-hydrocarbon group particularly if both H and D hydrogen isotopes are present in the SOL. The left side of Fig. 3 shows a hydrocarbon spectrum measured in the flat top phase of an ohmic discharge $\approx$ 1000 shots after last boronization resulting in a methane yield of 1.1%. The dominant $C_2D_xH_y$ hydrocarbons are acetylene $(x+y=2)$ and ethane $(x+y=4)$ with smaller contributions of ethane $(x+y=6)$. The overall C_2-hydrocarbon yield is estimated to be about 1% reaching an overall yield similar as methane and contribute thus twice to the carbon erosion. The right side of Fig. 3 shows a spectrum taken about 50 discharges after siliconization of TEXTOR for an NBI heated discharge with hydrogen fueling. The methane yield is about 0.6%, only half of that shown on the left side. More pronounced is the reduction of C_2-hydrocarbon formation — which is about a factor of ten. A strong reduced CO formation is observed demonstrating the beneficial effect of siliconization for oxygen gettering. C_3-hydrocarbons could not be detected at this scale. Thus incorporation of silicon can reduce the formation of higher hydrocarbons significantly and reduce the overall chemical erosion.

The C_2-yields show in general a tendency to increase with increasing plasma density, or decreasing plasma temperature as shown in Fig. 4. At the highest density the plasma detaches from the limiters resulting in a drop of the hydrogen flux.

Adding up methane and higher hydrocarbons the hydrogenic chemical carbon erosion yield (sum of eroded carbon atoms/hydrogen flux) observed by mass spectroscopy reaches values typically from 1.5 up to 4%. Similar overall hydrocarbon formation rates are measured by mass spectroscopy in the divertor exhaust of the ASDEX tokamak [25].

3.2. Optical spectroscopy, methane

Methane formation is usually studied by the band emission of the CH(D) radical at 431 nm. In TEXTOR methane formation yields are evaluated from CD and H_γ light using photon efficiencies of 100 and 1000 for CD and H_γ, respectively [26,27]. Similar values are used worldwide. Higher carbon ionization states have been observed in parallel in order to evaluate the contribution of the hydrocarbon source to the overall carbon release.

Several results on methane formation based on CH(D) spectroscopy in TEXTOR and other tokamaks have been published. In Asdex-U methane yields of 1% have been evaluated at the location of the inner wall graphite tiles [28] and a yield of 3% is reported from measurements in front of the divertor plates [29]. A methane yield of 1% is also observed based on the light emission inside the throat of the TORE-Supra actively cooled pumplimiter [30]. In these experiments target temperatures have been below

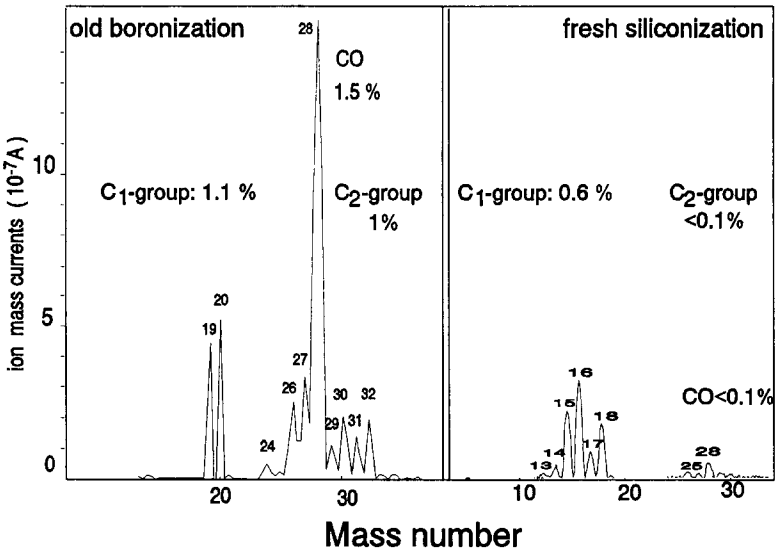

Fig. 3. Mass spectrum measured with the Sniffer probe for a deuterium filled discharge under old boronized wall conditions and about 20 discharges after fresh siliconization for a discharges with hydrogen fueling. The peak height of hydrogenic masses (2, 3, 4, not shown) are normalized to each other [33].

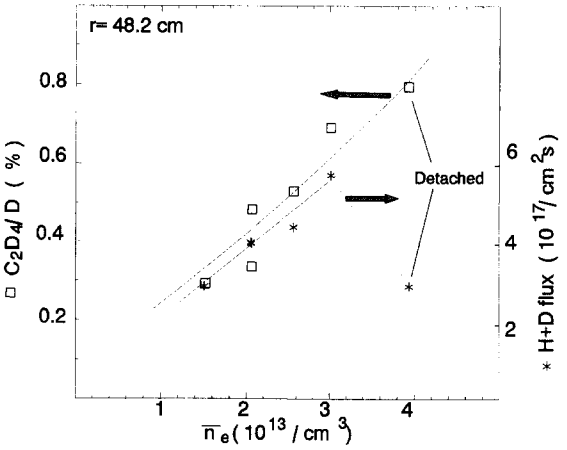

Fig. 4. Ethane formation yield ($C_2H_xD_y$, $x + y = 4$) and hydrogenic flux as function of line averaged density for ohmic discharges (target temperature < 150°C). At the highest density the plasma has detached from the limiters.

700 K and hydrogen flux densities ranged between $2 \times 10^{17}/cm^2$ s [28], $7 \times 10^{17}/cm^2$ s [29] up to $10^{19}/cm^2$ s [30]. In TEXTOR, most data have been obtained with the testlimiters at the LCFS [31]. In deuterium fueled discharges the methane yields range between 3 and 5%. Similar to mass spectroscopy the yields change little when varying the plasma density and thereby the hydrogen flux density, which ranges between $5 \times 10^{17}/cm^2$ s up to several $10^{18}/cm^2$ s. Inserting the limiters deeper into the plasma and using NBI heating the impinging flux densities have been increased up to several 10^{19} D/cm^2 s and the CD photon and corresponding methane yields decrease down to 1%. The decrease of the apparent methane yield with insertion of the limiter beyond the LCFS can be considered as an indication of a flux-dependent decrease of the methane formation. However, the local plasma temperatures increases under these conditions up to values of 80–100 eV resulting in high impact energies which also might decrease methane formation. This is suggested by laboratory experiments showing a decrease of methane formation for lower temperatures ($\lesssim 600$ K) and for particle impact energies exceeding about 250 eV [16]. Secondly, the radial extension of CD light emission becomes very narrow and part of the light is shadowed from the tangential view of the spectrometer. Last, CD photon efficiencies might not be appropriate under these plasma conditions.

The externally heatable limiter has been used in reproducible ohmic standard target plasmas ($\bar{n}_e = 2.5\ 10^{13}/cm^3$, n_e (46 cm) $= 3 \times 10^{12}/cm^3$, $T_e = 30$ eV) with the limiter tip at the LCFS (46 cm) [32]. The deuterium particle flux at the location of the spectrometer view is estimated to about 2×10^{18} D/cm^2 s. The experiments have been done during the first day after a fresh boronization resulting in large boron fluxes in the plasma edge. Spectroscopy of a BII and CII line in front of the limiter shows a B/C flux ratio of 1.2–0.8. Thus a B/C layer on top of the graphite surface is built on which the methane is formed. This results also in the appearance of emission light from the BH radical which will be discussed in [32]. The upper part of Fig. 5 shows the ratio of CD/H_γ light as a function of the limiter temperature. Only a slight increase of the methane formation (less then 50%) is observed from room temperature up to a temperature region extending from 450 to about 1050 K, in which the methane formation is nearly constant. Methane formation drops then for higher temperatures, reaching at 1400 K a yield of about 1/10 of its value at 600 K. The lower part of the figure shows recently measured methane formation obtained under 25, 100 and 250 eV energy hydrogen beam conditions at low flux densities for comparison [33]. Under TEXTOR conditions the temperature profile is much broader and the drop in methane formation towards higher temperatures is shifted by about 300 K to the higher temperatures as compared to the low-flux laboratory data. A shift of the maximum of the chemical peak towards higher temperatures for high flux conditions is already predicted by early models of hydrocarbon formation [34] and also by recent models

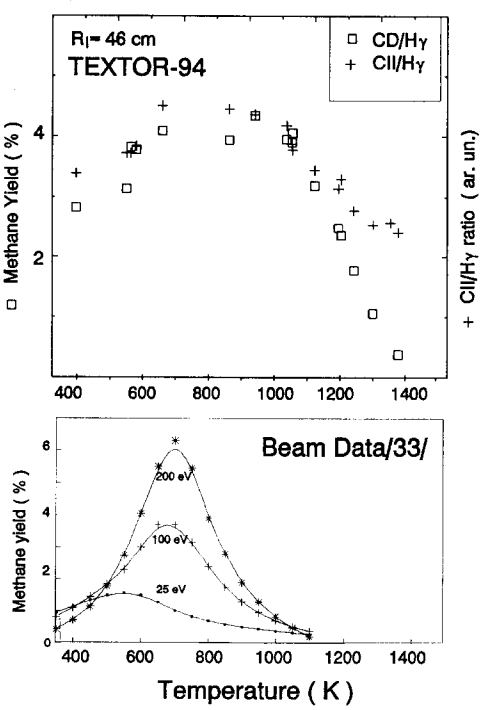

Fig. 5. Upper: CD/H_γ photon yield as function of limiter temperature for identical standard ohmic discharges with the limiter at the LCSF. The right scale shows absolute methane yields evaluated with photon efficiencies as described in text. The figure shows also the relative behaviour of a normalized CII (426.7 nm) line (CII/H_γ). Lower: recent measured beam data on methane formation at low impact energies under low beam flux conditions.

[14,15]. It can be understood as a decrease of the hydrogen concentration in the near surface of the carbon material. The maximum of chemical erosion extends up to 1050 K, which is well above the temperature of the chemical peak observed in low energy plasma experiments in PISCES at fluxes of 5×10^{17} H/cm^2 s (900 K, [35]). The data indicate thus that under the ITER divertor flux conditions the chemical peak may extend to even higher temperatures. Methane formation at lower temperatures (< 600 K) and low particle impact energies is significant and much stronger then expected from beam data at higher impact energies. This is also observed with the Sniffer probe. The presently assumed mechanism of hydrocarbon formation on graphite surfaces at lower temperatures is that the methane formation is a kinetic ejection of surface hydrocarbon complexes by collisional energy transfer. This is believed also to cause the observed isotope effect [16,19]. The left hand scale of Fig. 5(a) shows the absolute methane yields obtained using the photon yields mentioned above. As reported earlier from TEXTOR [31], the yields are between 3 and 4%. They are the same as for 'old' boronized wall conditions, where the boron fluxes are reduced at least by a factor of ten as compared to the conditions here.

The corresponding behavior of the ratio of CII (426.7 nm) to the H_γ line intensities is shown also in Fig. 5 (right hand scale). This ratio decreases by about 40% when the CD light vanishes at high surface temperatures. This shows that 40% of the CII ions in front of the limiter originate from the hydrocarbon source whereas the remaining CII ions at high surface temperatures must originate from physical sputtering by deuterium and carbon ion selfsputtering (oxygen fluxes under these conditions have been very low ($< 0.3\%$, fresh boronization)). The physical sputter yield of carbon for present conditions is estimated to be about 1.5%. Thus an overall hydrocarbon yield — including the contribution from higher hydrocarbons — of at least 1% has to be assumed in the temperature range between 400 and 1050 K in order to account for the decrease of 40% of the CII light at high temperatures. This value is a lower limit since some fraction of the emitted molecules are redeposited onto the surface before they reach the CII ionization state and emit light. As discussed in Section 4 Monte Carlo calculations indicate a mean value of the redeposition probability of 50% for the present conditions. With this value the intensity of the primary hydrocarbon source has to be increased to 2% to fit the decrease of 40% of C^+ light. However, as shown in Section 4 the redeposition probability is subject to large uncertainties.

3.3. Methane formation on metallic limiters

A remarkable behavior of the carbon and methane release has been observed for metallic limiters. Cu, SS, Mo and W limiters have been positioned at or 0.5 cm outside the LCFS in TEXTOR and methane release was observed as described above. The source of carbon on metallic limiters is the result of the deposition of carbon impurities flowing in the plasma boundary. In equilibrium (which is reached very rapidly) deposition and release balance and a resultant carbon surface concentration is established. It can be written as

$$F_c(1-R) = n_c(F_d \times Y_{dc} + F_i \times Y_{ic}),$$

where F_c, F_d, F_i are the impinging fluxes of carbon impurities, deuterium and other impurities (including carbon), Y_{dc}, Y_{ic} the erosion yields of carbon on the metallic surface by deuterium and impurity impact respectively, n_c the carbon surface concentration and R the reflection coefficient. At the LCFS the limiters are under erosion dominated conditions (no net carbon layer is growing) and n_c is in the submonolayer range. It has been reported earlier from TEXTOR that in front of SS and Cu limiters the CD/H_γ light efficiencies reaches values as high as 0.8, which would correspond (using the above mentioned photon efficiencies) to a methane yield of 8%, even higher than in front of a graphite limiter under similar conditions [31]. The ratio of the intensities and the radial decay length of CD and CII light in front of these limiters during plasma interaction has been found to be equal to those measured during puffing of small amounts of methane through a hole in the limiter. This indicates that most of the CII light during plasma interaction originates from methane. Those carbon impurities which stick to the surface and are not directly reflected recycle in the form of methane. This can only be the case if we assume that the carbon atoms which stick to the surface are rapidly hydrogenated and released as hydrocarbon molecules. This results in a low equilibrium surface carbon concentration ($\lesssim 10^{14}$ C/cm^2) and a negligible physical sputtering. With an estimated carbon impurity flux density at the LCFS of 10^{16}/cm^2 s, and an equilibrium surface concentration of carbon on the surface of $\leq 10^{14}$/cm^2 we obtain a surface residence time of 0.01 s which is much smaller then the confinement time of carbon impurities in the plasma.

The behavior is quite the opposite on molybdenum and tungsten limiters. There the CD light brightness is barely detectable and the yields are at least one order of magnitude lower, although the impinging carbon impurity fluxes are similar. A larger fraction of the impinging carbon impurities is directly reflected due to the larger mass but the fraction adhering on the surface is released by collisonal energy transfer. The marked difference between Cu, SS and Mo and W materials might be explained by the fact that Mo and W metals form a carbidic bond with impinging carbon, which is not known for Cu and SS.

No systematic study of higher hydrocarbon formation has yet been made in TEXTOR but some measurements of a C_2 band emission at 516.5 nm were performed. The C_2 band emission is only detectable at high plasma densities. CH_4 and C_2H_4 puffing has been performed to estimate

the ratio of methane to higher hydrocarbon emission under plasma impact and a value of 1/3 has been estimated. Some more information is given in [32].

3.4. Discussion of methane formation yields

The present data show still significant discrepancies of methane formation yields measured in different devices and with different techniques. Extrapolations of beam data to high flux conditions predict yields near 3–4%, if no decrease with flux is assumed, or near 1–2% assuming a weak decrease with flux as indicated by beam data and other observations. Mass spectroscopy in TEXTOR shows methane yields of 1–1.5%, while yields determined from optical emission spectroscopy are 3–4% with the limiter at the LCFS. Lower yields are only observed when the limiter is inserted inside the plasma beyond the LCFS. The decrease of the CII light of about 40% at high target temperatures, where hydrocarbons have disappeared, indicates in comparison with estimated physical sputter yields an overall hydrocarbon source of 1–2%, depending on the redeposition behavior. Furthermore, methane formation yields in front of steel and copper limiters positioned at the LCFS in TEXTOR reach values near 8%, which require an impinging carbon to hydrogen flux ratio of the same amount. Such carbon fluxes in the plasma edge are to high, indicating that methane yields in front of the metallic limiters are overestimated. There are thus several arguments indicating that the photon efficiencies for CD and H_γ light as mentioned above overestimate the methane formation. The overestimation might be estimated to be about a factor of two. The underlying reasons are not clear. First, photon efficiencies might not be correct. Next, local transport of hydrocarbon ions and -radicals in the near surface region can influence the amount of CD radicals, which are observed: some will be redeposited onto the surface and do not contribute to the CD molecular light. This would, however, underestimate the primary methane flux evaluated from the surviving CD radicals assuming that the redeposited species stick on the surface. If redeposited species are reflected, on the other hand, the CD light might be enhanced since the reflection allows for several attempts to radiate finally as CD radical. First calculations with a local Monte Carlo code show, however, that these effects can hardly account for a factor of two in the CD light emission for a given methane source intensity. We would also emphasize that any investigation of methane formation from CD and H_γ light intensity has to consider carefully the geometry of the spectroscopic view with respect to the source distribution of hydrogen and hydrocarbons. Since hydrogen atoms penetrate much deeper into the plasma than hydrocarbon molecules the CD light is restricted much more narrow to the surface than the H_γ light. Thus the spectroscopic view can observe light emitted from different areas.

4. Local transport and redeposition of hydrocarbon molecules

As important as the absolute hydrocarbon impurity release is the study of the local transport of the molecules. This influences the contribution of the hydrocarbon source to the carbon plasma impurity contamination and determines in particular the local erosion of the walls. Fig. 6 shows the radial intensity distributions of the CII light taken at two different temperatures: At the maximum of the chemical source at 600 K and at 1300 K where hydrocarbons have disappeared. The distributions show the decrease in the absolute light intensity at high temperatures but also that the additional CII light occurring in the maximum at 600 K appears predominantly close to the surface. The difference of both distributions must be attributed exclusively to contributions from hydrocarbon molecules to the CII light and is shown in the figure by the dashed line. The latter shows that the penetration of CII ions from a hydrocarbon source is much smaller than that from physically sputtered carbon atoms. This behavior is also seen by the local Monte Carlo calculations. The differences in the penetration depths indicate that the core fueling of carbon impurities originating from hydrocarbons is less (about 1/3 to 1/2) than that of sputtered atoms. Several observations in TEXTOR suggest that the impurity transport of low-Z elements under most of the conditions is diffusion dominated [36]. Under this condition the central impurity concentration is proportional to the ionization length and the flux intensity of the impurities [37]. Since the contribution of the hydrocarbons to the CII light is about 40%, their contribution to the central carbon impurity concentration would only be about 12–20% of the total C influx and thus not very significant. This estimate

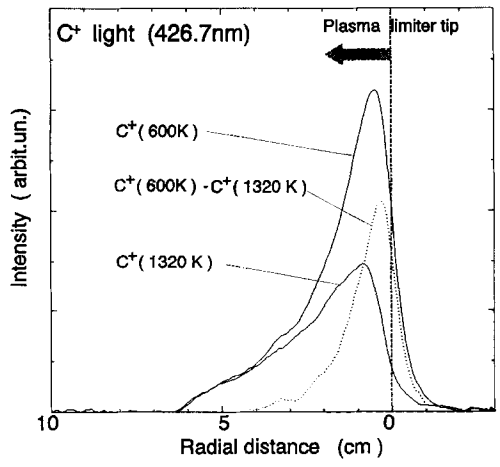

Fig. 6. Radial distribution of the CII light in front of the heated graphite limiter for limiter temperatures of 600 K (maximum of hydrocarbon formation) and 1320 K (no hydrocarbon formation). The dashed line shows the difference between both distributions.

is valid for the conditions where physical sputtering is a strong carbon source. It may explain observations in which the contribution of the hydrocarbon source to the global carbon impurity has been estimated from a global carbon impurity balance in the main plasma [38,39] concluding that physical sputtering together with some contribution from oxygen-induced carbon release is sufficient to explain the core carbon impurity concentration. However the hydrocarbon erosion contributes significantly to the target erosion and lifetime behavior of the walls and will probably dominate the carbon target erosion under the conditions predicted for the ITER divertor.

Transport and redeposition of methane have also been modelled by local Monte Carlo calculations (ERO-TEXTOR). The code is described in detail in Ref. [40]. The full testlimiter geometry is used, atomic data for methane are taken from the data published by Erhardt and Langer [41] and plasma profiles are taken from TEXTOR edge diagnostics. Physical sputtering of carbon is calculated according to the Bohdansky formula [12] and a constant methane formation yield of 2% has been used. Sputtered atoms are emitted with a cosine angular distribution and a Thompson energy distribution. Hydrocarbon molecules leave the surface with thermal energies and an isotropic angular distribution. Fig. 7 shows the total fraction of species returning back to the limiter surface as a function of the plasma temperature for two different edge densities. As can be seen, this fraction ranges between a lower value of 60% up to a maximum value of about 97% and does not depend strongly on plasma edge temperature. The curves show the deposition efficiency assuming that all species returning back to the surface stick. Fig. 8 shows the distribution of the redeposited species for these conditions. Redeposition occurs mainly by the ions of CD_4^+, CH_3^+ and CD_3 neutrals. The overall redeposition probability depends significantly on the sticking model of the redeposited species. In Fig. 7 it is shown that for the conditions measured for the heated limiter ($n_e = 2.5 \times 10^{12}/m^3$, $T_e = 30$ eV) the overall redeposition is 70% if all species stick on the surface. Redeposition decreases to 52% assuming that the ions stick with 50% and the neutrals with 0.5% probability and the reflected species are hydrogenated to saturated CH_4. The redeposition fraction is only 35% using the same sticking probabilities but assuming that the neutrals are reflected as they come in. Thus hydrogenation of the reflected radicals to saturated CH_4 or not influences significantly the overall redeposition. The fraction of the hydrocarbon molecules which are redeposited do not contribute to plasma contamination nor to the C^+ light emission. The intensity of the primary chemical source thus has to be enhanced to account for redeposition, as already discussed in Section 3.3.

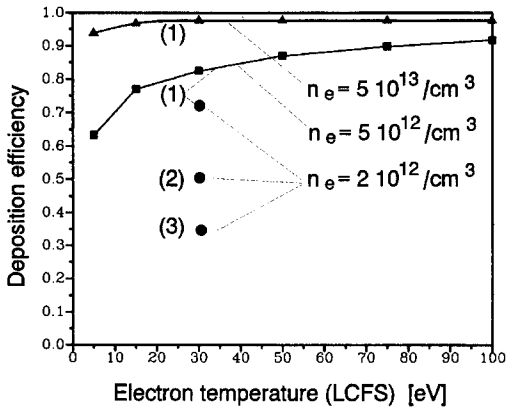

Fig. 7. Overall deposition efficiency of redeposited species originating from methane formation for different plasma densities and temperatures at the LCFS. The limiter tip is at the LCFS and the testlimiter geometry in TEXTOR is used. Plasma density and temperature profiles are taken from measured data and the a constant methane yield of 2% is used. Curves (1) assume a sticking fraction of 100% for redeposited species, point (2) 99.5% sticking for ions and 50% for neutrals and reflected neutrals are hydrogenated to CH_4. For point (3) it is assumed that reflected neutrals leave as they come in.

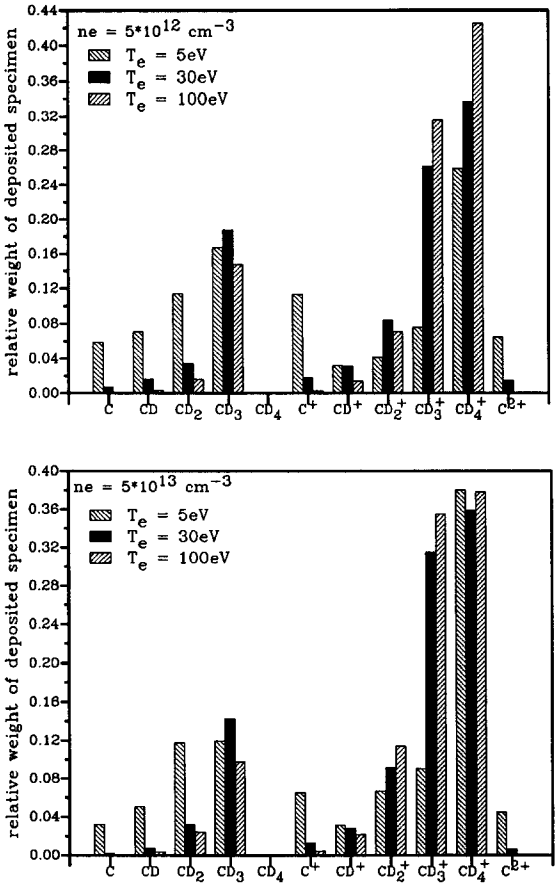

Fig. 8. Distribution of redeposited species for two different densities (as used in Fig. 7) and for different edge temperatures.

Puffing of methane, higher hydrocarbons and silane has been used to study experimentally the local transport and redeposition properties of the molecules in detail [40,42]. Some important results have been obtained:

The flow of ionic species does not follow the direction of the magnetic field lines. The pattern of deposited silicon and carbon during SiH_4 and CH_4 gas puffing is tilted with respect to the direction of the magnetic field. The pattern can be explained quantitatively by assuming a radial electric field leading to an $E \times B$ drift flow of the ionic species. This effect must be taken into account in order to calculate and predict the redeposition behavior in the vicinity of high erosion dominated areas.

Significant codeposition of carbon is observed in the deposited silicon layers. A fraction of C/Si of about unity has been measured post mortem for the layers deposited during SiH_4 injection on graphite as well as on metallic limiters. The latter observation shows that the codeposited carbon originates from the background flow of carbon impurities in the plasma edge. This background carbon flow is 'frozen in' in the growing silicon layer and a significant carbon codeposition occurs although no carbon layer is formed without local SiH_4 injection.

An important quantity for the discussion here is the deposition efficiency of carbon and silicon atoms injected as CH_4 and SiH_4 molecules. This has been determined from a comparison of the injected amounts and of the thicknesses and composition of the layers measured by in situ colorimetry and by post mortem surface analysis. It is only 4–7% in the case of silane injection [42,43] and a similarly small or even lower deposition efficiency is estimated for CH_4 puffing through a Cu-limiter. Such small deposition efficiencies are significantly lower compared with Monte Carlo calculations as described in the previous section. Several possibilities that would explain this behavior are under investigation and discussion presently. One possible reason which is being investigated is local electrical fields induced by ionization of the neutrals which act on the ionic species parallel to the magnetic field and drive the impurity ions away from the surface [44]. Another possibility might be that the erosion of the deposited material by plasma impact during the deposition process is significantly underestimated. Erosion of deposited material is presently included in the modeling by chemical and physical sputtering from the background plasma. Local gas injection may enhance the local erosion, for example due to CX neutrals. It might also be argued that the sticking probability of the redeposited species on the surface is much lower than presently assumed. However, unusually low sticking probabilities have to be used. No final explanation exists yet, but this discussion shows that the predictions on redeposition properties are subject to large uncertainties at the moment. The experimental database is small, many open questions exist and more detailed work is needed in order to make reliable predictions on redeposition for future devices.

5. Radiation enhanced sublimation

At graphite target temperatures above 1400 K ion beam experiments show that radiation enhanced sublimation (RES) of graphite is the dominated erosion channel [6,7,45,46]. Due to the expected RES-erosion of graphite in fusion machines, the working temperatures of carbon based materials are specified presently to stay below about 1400 K. However, measurements performed so far in TEXTOR on graphite testlimiters have shown that RES emission is negligible under these conditions. This observation is in agreement with observations in JET and TFTR [47–49], but contradictory observations have been reported [50]. The underlying physical reasons for the observed suppression of the RES emission in TEXTOR and in other tokamaks and for contradictory observations are not clear yet but clarification is necessary in order to make reliable predictions for different conditions. Several possibilities have been discussed [51] which might reduce or suppress the RES-erosion of carbon surfaces. Present understanding of RES is based on production of free carbon defects (interstitials) which diffuse and reach the surface and desorb in competition with annihilation at internal defects. This model predicts that the annihilation probability increases with increasing flux density leading to a decreasing probability of interstitials reaching the surface and thus decreasing RES-flux. The yield should decrease with the flux Φ as $\Phi^{-0.25}$ [52]. In earlier experiments performed in TEXTOR [52] heating of the limiters from room temperature up to 2000 K has been done by NI heated discharges within a duration of 2–3 s, which required deuterium flux densities in excess of $10^{19}/cm^2$ s. It was argued that these high fluxes reduce RES-emission in comparison to physical sputtering fluxes, the yield of which is independent of flux. It was also speculated that the fast rising transient temperatures may delay the onset of RES emission. To investigate these hypothesis carbon emission has been studied in TEXTOR-94 from a graphite limiter which has been preheated externally to about 1400 K, which is just the temperature of the onset of RES emission. The limiter surface was then heated up slowly by an ohmic target plasma up to a maximum temperature of about 1800 K at the end of the discharge (≈ 6 s). Fig. 9 shows the temporal behavior of the ratio of the CII/H_γ emission light and the development of the surface temperature near the location of the spectrometer. As can be seen, no significant increase of the CII light (514 m) intensity is observed during the discharge, although the limiter temperature rises continuously. This shows that the carbon release during the duration of the shot is constant and no additional RES erosion is measurable. The deuterium flux densities have been evaluated from power fluxes and H_γ light intensities to be about $2–3 \times 10^{18}/cm^2$ s, about one order of magnitude lower than in the earlier experiments on RES emission in TEXTOR. Plasma temperatures at the LCFS have been measured to be ≈ 30 eV which corresponds to ion impact

energies of ≈ 150 eV (sheath of $3kT_e + 2kT_e$ ($T_i = T_e$)). In Pisces RES has been observed at flux densities of 2×10^{17} H/cm^2 s at 250 eV target biasing with yields similar as in low flux, high energy beam experiments [54]. Fig. 10 [55–57] summarizes different RES emission observed in different devices as function of the impinging flux density by displaying the ratio of the carbon erosion at 1500 K (RES + physical sputtering) to that at 1200 K (only physical sputtering). Several data indicate a weak decrease of the RES yield with flux according to $\Phi^{-0.1}$ but the new data from TEXTOR-94 do not fit to this trend and call for a much stronger decrease with flux. Recent experiments with 5 keV argon bombardment of graphite have found a $\Phi^{-0.26}$ flux dependence of the RES yield in the flux range 10^{16}–10^{17} Ar/cm^2,s [53]. Accounting for the higher defect densities produced by 5 keV argon compared to deuterium, such stronger flux dependence of RES would be expected to occur under deuterium impact in the flux range between 10^{17}–10^{18} D/cm^2 s. The expected behavior is indicated in Fig. 10 by the dashed line. However, this is speculative and the new data may also indicate that the suppression of RES might not only be due to the high flux densities but to an additional parameter, which is not known at the moment. One speculation is that the spontaneous evaporation of free interstitials from the surface is hindered by the presence of (non carbon) surface impurity atoms. The present data have been obtained under freshly boronized wall conditions. Spectroscopy show a flux ratio of B/C of about 1/1 leaving the surface which should thus be similar in the near surface region. Further analysis is needed and will be done in TEXTOR-94.

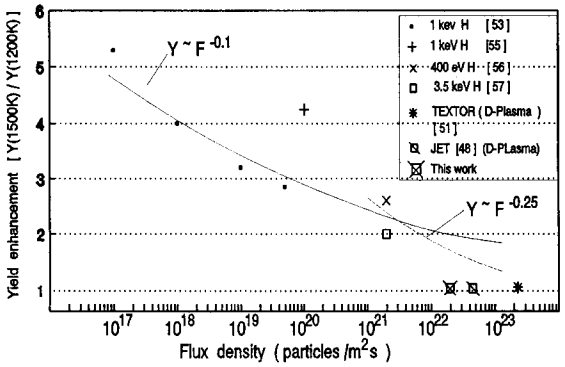

Fig. 10. Compilation of different data on RES emission for different experiments as function of flux density. Shown is the ratio of carbon emission at 1500 K to that at 1200 K (enhancement factor due to RES emission).

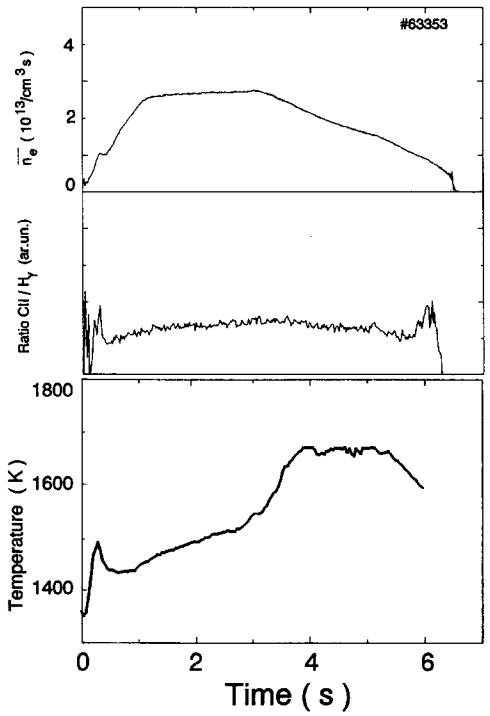

Fig. 9. Temporal evolution of the line averaged density (upper), the CII/H$_\gamma$ intensity ratio (CII light at 514 nm) and the surface temperature near the location of the spectrometer. The limiter was preheated externally to 1400 K and exposed to ohmic standard plasmas at the LCFS ($T_e = 30$ eV, $n_e = 2.5 \times 10^{12}$/cm^3).

6. Summary

Investigations of methane formation measured using mass spectroscopy in TEXTOR with the Sniffer probe give yields in the range of 0.8–1.2% at RT with a slight increase by a factor 1.5–2 at higher temperatures (600–900 K). The yield does not depend significantly on plasma edge conditions. Accurate evaluation of the contribution of higher hydrocarbons is more difficult and data show a larger scatter. Under carbon-dominated wall conditions in TEXTOR (old boronization or siliconization) the sum of the C_2 hydrocarbons reach similar yields to methane and thus dominate the carbon erosion. Siliconization and boronization do not decrease the methane formation significantly but a reduction of the C_2-hydrocarbon formation by more than a factor often has been observed after siliconization.

Optical spectroscopy on methane formation based on CD emission spectroscopy has been performed under various plasma edge conditions and with different limiters. Methane formation occurs in a broad temperature region extending up to 1300 K, much higher than observed in beam experiments. The yields increase from RT to a broad temperature region between 600–1300 K by a factor of about 1.5. Methane formation from a graphite limiter inserted in TEXTOR shortly after boronization (resulting in a C/B flux ratio emitted from the surface of 1/1) does not decrease the methane formation. Strong methane formation has been observed on Cu and SS limiters positioned at the LCSF while no CD light could be observed in

front of Mo and W limiters. The data show that carbon impurities from the background plasma recycle on Cu and SS in form of hydrocarbons whereas the carbon atoms which stick on Mo and W limiters are physically sputtered. Absolute methane yields obtained from optical spectroscopy range typically between 4% and 1%. With the limiters at the LCFS, the yields are 3–4% but decrease with inserting the limiters deeper into the plasma beyond the LCFS.

Observation of C^+ and C^{++} light in front of a heatable graphite limiter shows that about 40% of the light originates from the hydrocarbon source. Assuming a physical sputter yield of 1.5% this value implies that hydrocarbons are formed with a yield of 1% and of 2% including a redeposition probability of formed methane of 50% as indicated by Monte Carlo calculations.

The radial intensity distribution of CII light emission shows that the penetration of the C^+ light originating from the hydrocarbon molecules is much closer to the surface compared to the light from physically sputtered carbon. The smaller penetration suggests also a corresponding smaller fueling efficiency of the hydrocarbons.

Injection of methane, silane and higher hydrocarbons has been used to study the local transport of the molecules and, in particular, their redeposition behavior. The pattern and the amount of redeposited silicon and carbon after SiH_4 and CH_4 injection shows that the flow of the ionic species does not follow directly the magnetic field lines and is significantly tilted due, most likely, to the influence of local electric fields. Large amounts of carbon impurities from the background carbon impurity flow are incorporated in the deposited films. The overall deposition efficiency of injected silane and methane only reaches values between 4 and 7%.

Local Monte Carlo calculations show much larger redeposition efficiencies ranging between 60 and 90% if all species returning back to the surface sticks there. Increasing the reflection probability causes the redeposition efficiency to decrease down to 50 and 35%, depending whether reflected radicals are hydrogenated or not.

Observations on carbon release from an externally preheated graphite limiter which was then heated slowly further by plasma power flow in ohmic plasmas have been performed. The deuterium flux density was about $2 \times 10^{18}/cm^2$ s. No sign of an increasing carbon release with increasing surface temperature could be found showing that RES emission is negligible under these conditions.

References

[1] N. Noda, V. Philipps and R. Neu, these Proceedings, p. 227.
[2] J. Winter, J. Nucl. Mater. 176&177 (1990) 14.
[3] E. Vietzke, T. Tanabe, V. Philipps et al., J. Nucl. Mater. 145–147 (1987) 425.
[4] J. Winter, H.G. Esser, L. Könen et al., J. Nucl. Mater. 162–164 (1989) 582.
[5] J. Winter, H.G. Esser, G.L. Jackson et al., Phys. Rev. Lett. 71 (1993) 1549.
[6] J. Roth, J. Bohdanslry and K.L. Wilson, J. Nucl. Mater. 111&112 (1982) 775.
[7] V. Philipps, K. Flaskamp and E. Vietzke, J. Nucl. Mater. 111&112 (1982) 781.
[8] P. Wienhold, F. Weschenfelder and J. Winter, J. Nucl. Mater. 220 (1995) 452.
[9] P. Bogen, D. Rüsbüldt and U. Samm, J. Nucl. Mater. 162–164 (1989) 545.
[10] V. Philipps, A. Pospieszczyk, U. Samm et al., J. Nucl. Mater. 196–198 (1992) 1106.
[11] H. Bolt, R. Duwe, V. Philipps et al., J. Nucl. Mater. 212–215 (1994) 1239.
[12] J. Roth, E. Vietzke and A.A. Haasz, Atomic and Plasma–Material Interaction Data for Fusion, Vol. 1 (Int. Atom. Energy Agency, Vienna, 1991) (Suppl. to J. Nucl. Fusion) 63.
[13] A.A. Haasz and E. Vietzke, in: Physical Processes of the Interaction of Fusion Plasmas with Solids, eds. J. Roth and W. Hofer (Academic Press, New York, 1996) p. 135.
[14] J. Biener, U.A. Schubert, A. Schenk et al., J. Chem. Phys. 99 (1993) 3125.
[15] A. Schenk, B. Winter, J. Biener et al., J. Appl. Phys. 77 (1995) 2462.
[16] J. Roth and C. Garcia-Rosales, Nucl. Fusion, to be published.
[17] E. Vietzke, V. Philipps, K. Flaskamp et al., J. Nucl. Mater. 128&129 (1984) 545.
[18] E. Vietzke and V. Philipps, Fusion Technol. 15 (1989) 108.
[19] V. Philipps, E. Vietzke and M. Erdweg, J. Nucl. Mater. 162–164 (1989) 550.
[20] J. Roth, J. Nucl. Mater. 145–147 (1987) 87.
[21] Y. Hirooka, R. Conn, R. Causey et al., J. Nucl. Mater. 176&177 (1990) 473.
[22] C. Garcia-Rosales and J. Roth, J. Nucl. Mater. 196–198 (1992) 573.
[23] A.A. Haasz and J.W. Davis, J. Nucl. Mater. 175 (1990) 84.
[24] E. Vietzke, K. Flaskamp, V. Philipps et al., J. Nucl. Mater. 145–147 (1987) 443.
[25] W. Poschenrieder, K. Behringer, H.S.T. Bosch et al., J. Nucl. Mater. 220 (1995) 36.
[26] A. Pospieszcyk, Y. Ra, Y. Hirooka et al., Report UCLA-PPG-1251, Dec. 1989.
[27] K. Behringer, J. Nucl. Mater. 176&177 (1990) 606.
[28] A. Kallenbach, R. Neu and W. Poschenrieder, Nucl. Fusion 34 (1994) 1557.
[29] G. Lieder et al., Proc. 21th EPS Conf., Lisbon 1993, Europhys. Abstr. 18B Part II (1994) 722.
[30] Ch. Klepper, J.T. Hogan, L.W. Owen et al., Proc. 21st EPS Conf., Lisbon 1993, Europhys. Abstr. 17C, Part II 4–12.
[31] A. Pospieszczyk, V. Philipps, E. Casarofto et al., Proc. 22nd EPS Conf., Bournemouth 1995, Eurphys. Abstr. 19C Part II 309.
[32] A. Pospieszcyk, V. Philipps, E. Casarotto, U. Kögler, B. Schweer, B. Unterberg and F. Weschenfelder, these Proceedings, p. 833.
[33] J.W. Davis and A.A. Haasz, these Proceedings, p. 37.

[34] S.K. Erents, C.M. Braganza and G.M. McCracken, J. Nucl. Mater. 63 (1976) 399.
[35] D.M. Goebel, J. Bohdansky, R.W. Conn et al., Fusion Technol. 15 (1989) 102.
[36] B. Unterberg, V. Philipps, A. Pospieszczyk et al., Proc. 22th EPS Conf., Bournemouth 1995, Eurphys. Abstr. 19C Part II 305; these Proceedings, p. 93.
[37] W. Engelhardt and W. Fenneberg, J. Nucl. Mater. 76&77 (1978) 518.
[38] L. Horton and the JET team, in: Proc. 15th Int. Conf. on Plasma Physics and Controlled Nuclear Fusion Research, Seville, 1994, IAEA-CN-60/A-4-I-5.
[39] K. Ishimuzu, N. Hosogane, T. Takizuka et al., in: Proc. 15th Int. Conf. on Plasma Physics and Controlled Nuclear Fusion Research, Seville, 1994, IAEA-CN-60/D-P4-2.
[40] U. Kögler, J. Winter, H.G. Esser et al., Proc. 22th EPS Conf., Bournemouth 1995, Eurphys. Abstr. 19C Part IV 281; these Proceedings, p. 816.
[41] A.B. Ehrhardt and W.D. Langer, Report PPPL-2477 (Princeton University, Princeton, NJ, 1987).
[42] H.G. Esser, J. Winter, V. Philipps et al., J. Nucl. Mater. 220 (1995) 457.
[43] G. Mank, J.A. Boedo, P. Wienhold, H.G. Esser, K.H. Finken, L. Könen, A. Pospieszczyk, J. Rapp, J. Schwelberger, F. Weschenfelder and J. Winter, these Proceedings, p. 821.
[44] M.Z. Tokar, Contrib. Plasma Phys., to be published.
[45] A.A. Haasz and J.W. Davis, J. Nucl. Mater. 151 (1988) 77.
[46] R. Nygren, J. Bohdansky, A. Pospieszczyk et al., J. Nucl. Mater. 176&177 (1990) 445.
[47] D. Pasini, D.D.R. Summers and V. Philipps, J. Nucl. Mater. 176&177 (1990) 186.
[48] R. Reichle, D.D.R. Summers and M.F. Stamp, J. Nucl. Mater. 176&177 (1990) 375.
[49] A.T. Ramsey, C.E. Bush and H.F. Dylla, Nucl. Fusion 31 (1991) 1811.
[50] S.J. Tobin, J.T. Hogan, C. DeMichelis et al., Proc. 22th EPS Conf., Bournemouth 1995, Europhys. Abstr. 19C Part IV 345.
[51] V. Philipps, A. Pospieszczyk, B. Schweer et al., J. Nucl. Mater. 220 (1995) 467.
[52] V. Philipps, E. Vietzke, R.P. Schorn and H. Trinkaus, J. Nucl. Mater. 155–157 (1988) 319.
[53] Y. Ueda, K. Nakano, Y. Ohtsuka, M. Isobe, S. Goto and M. Nishikawa, J. Nucl. Mater. 227 (1996) 251.
[54] A.A. Haasz and J.W. Davis, J. Nucl. Mater. 151 (1988) 77.
[55] J. Roth, J. Bohdansky and K.L. Wilson, J. Nucl. Mater. 111&112 (1982) 775.
[56] Y. Hirooka, R. Conn, R. Causey et al., J. Nucl. Mater. 176&177 (1990) 473.
[57] A.A. Haasz, J.W. Davis, C.D. Grossmann et al., J. Nucl. Mater. 173 (1990) 108.